HHS Public Access

Author manuscript

J Orthop Res. Author manuscript; available in PMC 2019 October 01.

Published in final edited form as:

J Orthop Res. 2018 October ; 36(10): 2771–2779. doi:10.1002/jor.24028.

Quantitative MRI correlates with histological grade in a percutaneous needle injury mouse model of disc degeneration

Matthew Piazza[1], **Sun H. Peck**[1,2,3], **Sarah E. Gullbrand**[1,2,3], **Justin R. Bendigo**[1,2,3], **Toren Arginteanu**[1], **Yejia Zhang**[2,3,4], **Harvey E. Smith**[2,3], **Neil R. Malhotra**[1,2,*], and **Lachlan J. Smith**[1,2,3,*]

[1]Department of Neurosurgery, Perelman School of Medicine, University of Pennsylvania, Philadelphia, PA, USA

[2]Department of Orthopaedic Surgery, Perelman School of Medicine, University of Pennsylvania, Philadelphia, PA, USA

[3]Translational Musculoskeletal Research Center, Philadelphia VA Medical Center, Philadelphia, PA, USA

[4]Department of Physical Medicine and Rehabilitation, Perelman School of Medicine, University of Pennsylvania, Philadelphia, PA, USA

Abstract

Low back pain due to disc degeneration is a major cause of morbidity and health care expenditures worldwide. While stem cell-based therapies hold promise for disc regeneration, there is an urgent need to develop improved *in vivo* animal models to further develop and validate these potential treatments. The objectives of this study were to characterize a percutaneous needle injury model of intervertebral disc degeneration in the mouse caudal spine, and compare two non-invasive quantitative imaging techniques, microcomputed tomography and magnetic resonance imaging (MRI), as effective measures of disc degeneration in this model. Percutaneous needle injury of mouse caudal discs was undertaken using different needle sizes and injury types (unilateral or bilateral annulus fibrosus (AF) puncture). Mice were euthanized 4 weeks post-injury, and microcomputed tomography and MRI were used to determine T2 relaxation time of the NP and disc height index, respectively. Disc condition was then further assessed using semi-quantitative histological grading. Bilateral AF puncture with either 27 or 29G needles resulted in significantly lower T2 relaxation times compared to uninjured controls, while disc height index was not significantly affected by any injury type. There was a strong, inverse linear relationship between histological grade and NP T2 relaxation time. In this study, we demonstrated that quantitative MRI can detect disc degeneration in the mouse caudal spine 4 weeks following percutaneous needle

[*]Correspondence:, Lachlan J. Smith, Ph.D., Department of Neurosurgery, University of Pennsylvania, 110 Stemmler Hall, 3450 Hamilton Walk, Philadelphia, PA, 19104; Neil R. Malhotra, M.D., Department of Neurosurgery, University of Pennsylvania, 3rd Floor Silverstein Pavilion, 3400 Spruce St, Philadelphia, PA, 19104.

Author Contributions: M.P. designed and performed experiments, and drafted the manuscript. S.H.P. contributed to experimental design and performed experiments. S.E.G., J.R.B. and T.A. performed experiments. Y.Z. and H.E.S. provided conceptual input on experimental design. N.R.M. performed surgeries and designed experiments. L.J.S. designed experiments and drafted the manuscript. All authors reviewed the manuscript prior to submission.

The authors have no conflicts of interest to disclose.

injury, and may therefore serve as a surrogate for histology in longitudinal studies of both disc degeneration and cell-based therapies for disc regeneration using this model.

Keywords

Small animal model; intervertebral; disc height index; magnetic resonance imaging; T2 relaxation time

Introduction

Low back pain secondary to disc degeneration is a major cause of morbidity, lost productivity, and health care expenditures worldwide.[1-6] Conservative treatments consist of pain medications and physical rehabilitation. Fusion surgery for refractory cases is largely destructive in nature, alters the normal biomechanics of the spine, has limited efficacy, and may increase the risk of adjacent level disease.[7,8] There is an urgent need to develop new regenerative therapies that not only alleviate symptoms but also restore disc structure and function.

Injectable, biological treatment strategies, such as stem cells, hold significant promise in this regard; however, effective experimental study of such therapies requires an animal model that recapitulates the mild to moderate disc degeneration that would be targeted in human patients. While large animal model evaluation is a requisite preclinical step, initial *in vivo* mechanistic and screening studies necessitate the use of small animal models such as mice, where established techniques in genetic manipulation permit mechanistic studies of stem cell-mediated regeneration, and lower costs enable higher throughput experimentation.[9-11]

Most small animal models of disc degeneration have utilized rabbits[12-21] or rats,[22-29] as the size scale of mice presents greater technical challenges. One of these challenges is the risk of inducing severe degeneration, in which there is complete loss of healthy nucleus pulposus (NP) tissue, biomechanical integrity, and normal disc height, which is not well-suited for studying the regenerative properties of cell-based therapies.[30] Most published small animal models have adopted an open approach in which an incision and soft tissue dissection are utilized to expose the disc space.[30-32] Developing an injury system for inducing milder degeneration that minimizes interruption of surrounding tissue architecture may produce a more physiologic model and reduce scarring that may impair cell delivery. A percutaneous needle injury approach may achieve this goal[33] but has not been studied extensively in mice. Additionally, identifying the optimal injury size to induce moderate disc degeneration is critical and has only been studied in mice to a limited extent.[34]

Validation of robust, non-invasive, quantitative techniques for assessing disc condition in mouse models of disc degeneration is essential to maximize the utility of these models in the study of therapeutics. Sensitive imaging techniques that measure clinically meaningful metrics such compositional changes and loss of disc height are of particular value but are challenging to implement in mice due to size constraints. Previously, microcomputed tomography (μCT) has been applied successfully to measure volumetric disc height changes in a mouse model of severe disc degeneration.[30] Quantitative magnetic resonance imaging

(MRI) has been successfully applied to assess disc condition in humans and a range of animal models, including rats.[27,35-37] T2 relaxation time, specifically, has been validated as an effective surrogate for disc composition, including hydration state and proteoglycan content.[38-40] To our knowledge, few studies have applied quantitative MRI to determine T2 relaxation values to assess disc condition in murine models,[37] and none, to our knowledge, have done so in mice.

The first objective of this study was to optimize a percutaneous needle injury model of intervertebral disc degeneration in the mouse caudal spine, and specifically, to investigate the relationship between needle size, unilateral or bilateral annulus fibrosus (AF) puncture, and degenerative grade in this model. The second objective was to compare two, non-invasive quantitative imaging techniques, μCT and MRI, as effective surrogates for disc degeneration in the mouse caudal spine confirmed through semi-quantitative histological grading.

Methods

Animals and Surgical Procedure

Animal studies were approved by the Institutional Animal Care and Use Committee of the University of Pennsylvania. Adult male C57BL/6 mice (31 mice, aged 6-8 months) were obtained from Jackson Laboratories (Bar Harbor, ME, USA). Surgeries were performed at the C7/8 and C9/10 levels of the caudal spine with standard aseptic technique, with each level randomly assigned to one of six different injury types (n=10 discs per group, Figure 1A). Either 31G, 29G, or 27G custom made needles with a 45° bevel (Hamilton Company; Reno, NV, USA) were utilized (Figure 1B) and inserted into the NP through a unilateral annular puncture or through the AF, NP, and the contralateral AF (bilateral puncture) under fluoroscopic guidance (Figure 1C). Injured levels were marked on the adjacent skin using ink tattoo. The C8/9 levels served as intervening controls (n=30). Following surgeries, animals were returned to their cages, resumed normal activity, and were euthanized 4 weeks later. Mouse tails were then removed via sharp dissection, sealed in plastic to prevent dehydration, and frozen at -20°C. Importantly, the imaging studies described below were undertaken with skin and other surrounding tissue intact, in order to minimize unintended trauma to the disc space that might confound results.

Magnetic Resonance Imaging

Frozen mouse tails were thawed, sealed in plastic wrap and imaged on a 4.7T MRI scanner. Scans were performed using a DDR console (Agilent; Palo Alto, CA, USA) interfaced to a 4.7T horizontal bore magnet (Magnex Scientific Limited; Abington, UK) using a custom-made 11 mm diameter solenoid coil. A series of mid-coronal slices for T2 mapping (TE = I*11.14 ms, I = 1,2,3,…16; 16 echo times in total) were obtained with an in-plane resolution of 97.7 μm and a 0.5 mm slice thickness. The bandwidth was 100 kHz. T2 maps of one mid-coronal slice from each sample were then generated in ImageJ in a pixel-wise fashion using a simplex algorithm (MRI Analysis Calculator plugin, NIH, Bethesda, MD). The NP region was then manually contoured to calculate mean T2 values. To maintain consistency between samples, the NP base was defined as a central 9-pixel wide region. Average T2 maps of the

intervertebral discs in each experimental group were generated using custom Matlab software, as previously described.[35,36] Briefly, for each individual T2 map, the disc was manually segmented and, using principle component analysis, T2 maps linearly transformed to a fixed dimension grid with regularly spaced points within a rectangular coordinate system. Once mapped to a standardized grid, T2 values could be averaged among experimental groups on a pixel-by-pixel basis. To confirm the reproducibility of this MRI technique, one uninjured caudal disc from one additional 6 month old C57BL/6 mouse was imaged three successive times. In between scans, the tail was removed from the coil and the coil was removed from the scanner, then both were repositioned. Nucleus pulposus T2 relaxation time was calculated for each scan, and the mean, standard deviation and coefficient of variation were calculated.

Microcomputed Tomography

Microcomputed tomography (μCT) imaging was performed on mouse tails at 10 μm isotropic resolution (300 ms integration time, 55kVp, 72 microA) using a μCT50 scanner (Scanco; Brüttisellen, Switzerland). Volumetric calculations of disc height for experimental levels and intervening controls were performed in Matlab (V9.2.0; Mathworks; Natick, MA, USA) using a custom program adapted from a previous method.[30] Disc height was calculated as the distance between the superior endplate and inferior endplate averaged over the entire disc. Average proximal vertebral body height was measured in a similar fashion and defined as the sum of average superior endplate, inferior endplate, and mid-vertebral body measurements. To calculate disc height index (DHI), average disc height was divided by the average height of the proximal vertebral body.

Histological Assessment

Following MRI and μCT imaging, mouse tails were fixed for 5 days in buffered 10% formalin and decalcified (Formical 2000; Decal Chemical Corporation; Tallman, NY, USA) as assessed by radiography. Samples were processed into paraffin and sectioned at 7 μm thickness. Mid-coronal sections were double-stained either with Alcian blue and picrosirius red (AB&PR) to demonstrate glycosaminoglycans and collagens, respectively, or hematoxylin and eosin (H&E) to evaluate disc morphology and cellularity. Blinded semi-quantitative grading of slides for both stains was performed by three assessors (M.P., S.E.G. and L.J.S.) using a continuous scale (Table 1) adapted from Gullbrand et al. and Masuda et al.[15,41] The grading scale assesses four properties of the disc (AF organization, AF/NP border, NP extracellular matrix (ECM) content, and NP cellularity) and scored from 0 to 100 with greater scores indicating worse histological grade (i.e. more degenerate disc). A total score is calculated by summing each category (0 to 400). Prior to grading, blinding was accomplished by assigning a random number from 0 to 100 to each AB&PR and H&E section. Individual subcategory and total scores of the reviewers were averaged prior to statistical analysis.

Statistical Analysis

Where data were normally distributed, as assessed by the Shapiro-Wilk test for normality, statistical differences between study groups were established using one-way analyses of variance (ANOVA), and data was presented as mean ± standard deviation (SD). For absolute

disc height and DHI, to account for inter-animal differences in disc size that might add variability to these outcomes, a generalized linear model was used with animal included as a random variable to control for this potential confounder. Where data were not normally distributed, Kruskall-Wallis multiple comparisons tests were performed (specifically, for histologic grading analysis), and data was presented as median and interquartile range (IQR). Where appropriate, Dunnett's test was performed to establish pair-wise significant differences between injury groups and the control group. Inter-assessor reliability was assessed using the intraclass correlation coefficient. Linear regression analysis was used to establish significant correlations between histologic grade and imaging outcome metrics. Correlation strength was defined as follows: $r > 0.7$ as strong, $0.4 < r < 0.7$ as moderate, and $r < 0.4$ as weak. In all cases, significance was defined as $p < 0.05$. All statistical analyses were performed using SPSS (IBM; Armonk, NY, USA).

Results

Magnetic Resonance Imaging

All animals successfully underwent surgeries, survived the duration of the study, and were sacrificed for post-mortem analyses at 4 weeks post-surgery. Representative echoes illustrating T2 relaxation times for a control disc and a disc that received a bilateral injury with a 27G needle are shown in Figure 2A. T2 relaxation times for the NP differed significantly among experimental groups ($p=0.001$; Figure 2B). Post-hoc analyses revealed that 27G and 29G bilateral puncture (T2: 56.3±9.7 ms and 58.7±10.5 ms, respectively) demonstrated significantly lower T2 values compared with uninjured controls (T2: 67.4±5.2 ms; $p=0.004$ and $p=0.038$, respectively) compared to control. Composite T2 MRI maps for each experimental group are shown in Figure 2C. Reproducibility of the MRI technique was confirmed by imaging one uninjured caudal disc three successive times. Nucleus pulposus T2 relaxation time was 75.3 ± 2.8 ms, which corresponds to a coefficient of variation of 3.8%.

Microcomputed Tomography

Disc height index was not significantly different between experimental groups (Figure 3). Similarly, for absolute disc height measurements, there were no significant differences between injury and control groups. A generalized linear model, with AF puncture type (unilateral or bilateral) and needle size as fixed factors, did demonstrate that puncture presence and type had a significant effect on DHI ($p=0.018$). The effect of animal on disc height overall was significant ($p<0.001$). Adjusted DHI for control, unilateral AF puncture, and bilateral AF puncture were 0.111 ± 0.016, 0.114 ± 0.016, and 0.105 ± 0.014, respectively.

Histological Assessment

Blinded semi-quantitative histological assessment revealed overall differences in histologic grade between experimental groups ($p = 0.002$; Figure 4A). Specifically, post-hoc analysis revealed that 29G and 27G bilateral puncture injury resulted in significantly worse overall histologic grade (262.1 (IQR: 119.4-306.8) and 330.0 (IQR: 222.3-372.8), respectively) compared to control (57.7 (IQR: 45.3-81.8), $p = 0.003$ and $p = 0.018$). When examining

each individual categorization of the histological score (Figure 4B-E), there were overall differences between experimental groups for AF organization ($p = 0.001$), AF/NP border ($p < 0.001$), NP ECM content ($p < 0.001$), and NP cellularity ($p < 0.001$). Again, post-hoc analysis for each of these subcategories, with the exception of the NP ECM score, revealed significantly worse scores between 27G and 29G bilateral puncture injuries and control: AF organization, $p = 0.002$ and $p = 0.010$; AF/NP border, $p = 0.005$ and $p = 0.045$; NP ECM, $p = 0.024$ and $p = 0.062$; and NP cell $p = 0.003$ and $p = 0.021$, respectively. Intraclass correlation coefficients for total histologic, AF organization, AF/NP border, NP matrix content, and NP cellularity scores were all greater than 0.95 ($p < 0.001$) indicating a strong correlative relationship among reviewers' scores. Figures 5 and 6 show H&E and AB&PR stained sections for samples corresponding to the best, median, and worst overall histological grades for each experimental group. There was a strong, significant inverse linear correlation between NP T2 relaxation time and overall histological grade ($r=0.70$, $p<0.001$; Figure 7A), while a weak but still significant, inverse correlation existed between DHI and histologic grade ($r = 0.23$, $p = 0.031$; Figure 7B).

Discussion

In this study, we optimized a novel, percutaneous caudal disc injury model for disc degeneration in the mouse. This work enhances and extends previous work that demonstrated that a percutaneous injury (26G needle) can successfully initiate histologically identifiable degeneration in mouse caudal discs.[33] We have established the threshold needle size and puncture type required to generate disc changes detectable by both quantitative MRI and semi-quantitative histology (bilateral AF puncture with a 29 or 27G needle). Of note, while bilateral AF puncture resulted in NP changes consistent with degeneration, including shorter T2 relaxation times and histological changes, it did not induce statistically significant alterations in disc height compared to controls. The histological changes reported (lamellar disorganization, decreased cellularity, and altered in the NP) are consistent with prior needle injury models of disc degeneration in the mouse.[30,32,33] Unilateral puncture with any needle size was not able to elicit statistically significant degenerative changes as assessed by either MRI or histologic grade. This finding contrasts with prior mouse needle injury models in which loss of disc height was observed.[30,32] Prior studies used an open surgical approach to expose the AF surface prior to injury. Our findings may suggest that a less invasive percutaneous injury technique, that preserves adjacent skin, muscle and tendon structure, and likely minimizes local scarring and inflammation, may result in milder degenerative changes. It is also possible that allowing degeneration to progress for longer than 4 weeks may result in greater disc height changes.

Non-invasive approaches to assessing disc condition that correlate with clinically meaningful metrics (such compositional changes and loss of disc height) are critical outcome measures for the successful application of small animal models in the study of disc degeneration and associated therapies. The small size of the mouse disc likely makes the effective application of standard non-invasive metrics for assessing disc degeneration, such as subjective Pfirrmann grading from MRI, and disc height changes from two dimensional and low resolution plain radiographs challenging and insensitive. While a correlation between T2 signal intensity within the NP and histological grade has been previously

demonstrated in a mouse model of disc degeneration,[31] as well as other small animal models,[19,27] the present study is the first to successfully apply quantitative MRI, using T2 relaxation times, to assess disc degeneration in a mouse model. Importantly, our findings demonstrate a strong, inverse linear relationship between histological grade and NP T2 relaxation time, a surrogate for tissue hydration and proteoglycan content.[38] This suggests that quantitative MRI imaging can be utilized *in vivo* as an effective non-invasive surrogate for histological changes in longitudinal studies of disc degeneration and regeneration.

Quantitative MRI of the mouse disc is not without its challenges. Population average T2 maps of the whole discs (Figure 3) revealed an area of low signal within the central portion of the NP in control discs which abates with more aggressive injuries, although incompletely. This area of low signal is associated with the cell-rich notochordal remnant that persists in the healthy adult mouse disc, and histological analysis revealed a decrease in NP cellularity with more aggressive injuries (Figure 4). Hence, quantitative T2 imaging of the NP may be less sensitive at detecting very mild injury, in which disappearance of the cell-dense region of the notochordal remnant may lead to an increase in the average T2 values in the NP, even with concomitant mild dehydration and proteoglycan loss. This may explain the higher (non-significant) T2 values for the 31G unilateral puncture group compared to control.

The percutaneous injury technique, which relies on fluoroscopic guidance for accurate needle placement, and does not permit direct visualization of the AF surface, is also not without challenges. While histological analysis revealed significant differences in degenerative grade between 29G and 27G bilateral puncture and control groups overall, there was still substantial variation within each experimental group. It was observed that each group had at least one nearly histologically normal intervertebral disc (Figures 5 and 6). A possible explanation for this variability is inconsistent needle placement. For example, a needle that passes obliquely through the AF my not result in NP depressurization. This underscores the importance of utilizing robust non-invasive *in vivo* imaging that can confirm the existence of degenerative changes for injured discs prior to delivering therapies.

This study has a number of limitations. First, biomechanical changes, as a consequence of degeneration, were not assessed. However, previous work has demonstrated that puncture of the mouse disc with a 26G needle resulted in only acute, non-progressive, significant biomechanical changes in compression and torsion.[30] Second, in the current study we did not discriminate between those degenerative changes that occurred due to traumatic injury and those which occurred subsequent to injury, driven by biological processes. In particular, establishing inflammation as an active mediator of progressive degenerative changes in this model would further enhance its physiological relevance. Third, we examined only one time point (4 weeks post injury), and it is possible that, while we were able to detect degenerative changes on MRI and histology for the 27G and 29G bilateral injury groups, these changes may have progressed further and/or other injury groups may have exhibit detectable degenerative changes if additional, later time points were also assessed. Future studies will utilize *in vivo* quantitative MRI to assess degeneration that occurs over time. Fourth, in this study we did not perform quantitative biochemical assays to determine GAG content within the NP, and our assessments of ECM changes were limited to histological evaluations.

Finally, all imaging was performed *ex vivo*; however, given that significant care was taken to minimize disruption to tissue structure and composition, we expect our results to be comparable to those obtained *in vivo*.

Conclusions

In the present study, we demonstrate that quantitative MRI can detect disc degeneration after percutaneous needle puncture, specifically after 29G and 27G bilateral AF puncture, when compared with uninjured controls. Semi-quantitative histological assessment confirmed MRI findings and strongly correlated with NP T2 values. This important result suggests that *in vivo* quantitative MRI may serve as a surrogate for histology in longitudinal studies of both disc degeneration and cell based therapies for disc regeneration in mice. Interestingly, DHI exhibited only subtle changes, suggesting that this percutaneous injury technique results in mild to moderate degrees of degeneration and may be well-suited for studying cell based therapies in which residual endogenous NP cells persist and paracrine signaling is still possible. Future studies will focus on applying this model to investigate cell-based therapies for disc regeneration.

Acknowledgments

Funding for this work was received from the National Institutes of Health (R21AR070959 and F32AR071298), the Department of Veteran's Affairs (I01RX001321), the Catherine D. Sharpe Foundation and the Penn Institute on Aging. Additional support was received from the Penn Center for Musculoskeletal Disorders (P30AR069619) and the Department of Neurosurgery at the University of Pennsylvania.

References

1. Dagenais S, Caro J, Haldeman S. A systematic review of low back pain cost of illness studies in the United States and internationally. Spine Journal: Official Journal of the North American Spine Society. 2008; 8:8–20.
2. Ekman M, Jonhagen S, Hunsche E, et al. Burden of illness of chronic low back pain in Sweden: a cross-sectional, retrospective study in primary care setting. Spine (Phila Pa 1976). 2005; 30:1777–1785. [PubMed: 16094281]
3. Juniper M, Le TK, Mladsi D. The epidemiology, economic burden, and pharmacological treatment of chronic low back pain in France, Germany, Italy, Spain and the UK: a literature-based review. Expert Opin Pharmacother. 2009; 10:2581–2592. [PubMed: 19874246]
4. Katz JN. Lumbar disc disorders and low-back pain: socioeconomic factors and consequences. J Bone Joint Surg Am. 2006; 88(2):21–24. [PubMed: 16595438]
5. Martin BI, Deyo RA, Mirza SK, et al. Expenditures and health status among adults with back and neck problems. JAMA. 2008; 299:656–664. [PubMed: 18270354]
6. Vos T, Flaxman AD, Naghavi M, et al. Years lived with disability (YLDs) for 1160 sequelae of 289 diseases and injuries 1990-2010: a systematic analysis for the Global Burden of Disease Study 2010. Lancet. 2012; 380:2163–2196. [PubMed: 23245607]
7. Eck JC, Sharan A, Ghogawala Z, et al. Guideline update for the performance of fusion procedures for degenerative disease of the lumbar spine. Part 7: lumbar fusion for intractable low-back pain without stenosis or spondylolisthesis. J Neurosurg Spine. 2014; 21:42–47. [PubMed: 24980584]
8. Zhang C, Berven SH, Fortin M, et al. Adjacent Segment Degeneration Versus Disease After Lumbar Spine Fusion for Degenerative Pathology: A Systematic Review With Meta-Analysis of the Literature. Clin Spine Surg. 2016; 29:21–29. [PubMed: 26836484]
9. Marfia G, Campanella R, Navone SE, et al. Potential use of human adipose mesenchymal stromal cells for intervertebral disc regeneration: a preliminary study on biglycan-deficient murine model of chronic disc degeneration. Arthritis Res Ther. 2014; 16:457. [PubMed: 25293819]

10. Tam V, Rogers I, Chan D, et al. A comparison of intravenous and intradiscal delivery of multipotential stem cells on the healing of injured intervertebral disk. J Orthop Res. 2014; 32:819–825. [PubMed: 24578095]
11. Yang F, Leung VY, Luk KD, et al. Mesenchymal stem cells arrest intervertebral disc degeneration through chondrocytic differentiation and stimulation of endogenous cells. Mol Ther. 2009; 17:1959–1966. [PubMed: 19584814]
12. Aoki Y, Akeda K, An H, et al. Nerve fiber ingrowth into scar tissue formed following nucleus pulposus extrusion in the rabbit anular-puncture disc degeneration model: effects of depth of puncture. Spine (Phila Pa 1976). 2006; 31:E774–780. [PubMed: 17023838]
13. Kong MH, Do DH, Miyazaki M, et al. Rabbit Model for in vivo Study of Intervertebral Disc Degeneration and Regeneration. J Korean Neurosurg Soc. 2008; 44:327–333. [PubMed: 19119470]
14. Lei T, Zhang Y, Zhou Q, et al. A novel approach for the annulus needle puncture model of intervertebral disc degeneration in rabbits. Am J Transl Res. 2017; 9:900–909. [PubMed: 28386320]
15. Masuda K, Aota Y, Muehleman C, et al. A novel rabbit model of mild, reproducible disc degeneration by an anulus needle puncture: correlation between the degree of disc injury and radiological and histological appearances of disc degeneration. Spine (Phila Pa 1976). 2005; 30:5–14. [PubMed: 15626974]
16. Sobajima S, Shimer AL, Chadderdon RC, et al. Quantitative analysis of gene expression in a rabbit model of intervertebral disc degeneration by real-time polymerase chain reaction. Spine Journal: Official Journal of the North American Spine Society. 2005; 5:14–23.
17. Chan DD, Khan SN, Ye X, et al. Mechanical deformation and glycosaminoglycan content changes in a rabbit annular puncture disc degeneration model. Spine (Phila Pa 1976). 2011; 36:1438–1445. [PubMed: 21270702]
18. Gregory DE, Bae WC, Sah RL, et al. Disc degeneration reduces the delamination strength of the annulus fibrosus in the rabbit annular disc puncture model. Spine Journal: Official Journal of the North American Spine Society. 2014; 14:1265–1271.
19. Chai JW, Kang HS, Lee JW, et al. Quantitative Analysis of Disc Degeneration Using Axial T2 Mapping in a Percutaneous Annular Puncture Model in Rabbits. Korean J Radiol. 2016; 17:103–110. [PubMed: 26798222]
20. Kim DW, Chun HJ, Lee SK. Percutaneous Needle Puncture Technique to Create a Rabbit Model with Traumatic Degenerative Disk Disease. World Neurosurg. 2015; 84:438–445. [PubMed: 25886720]
21. Zhou RP, Zhang ZM, Wang L, et al. Establishing a disc degeneration model using computed tomography-guided percutaneous puncture technique in the rabbit. J Surg Res. 2013; 181:e65–74. [PubMed: 22878152]
22. Cunha C, Lamas S, Goncalves RM, et al. Joint analysis of IVD herniation and degeneration by rat caudal needle puncture model. J Orthop Res. 2017; 35:258–268. [PubMed: 26610284]
23. Issy AC, Castania V, Silveira JW, et al. Does a small size needle puncture cause intervertebral disc changes? Acta Cir Bras. 2015; 30:574–579. [PubMed: 26352338]
24. Jeong JH, Jin ES, Min JK, et al. Human mesenchymal stem cells implantation into the degenerated coccygeal disc of the rat. Cytotechnology. 2009; 59:55–64. [PubMed: 19363673]
25. Zhang H, La Marca F, Hollister SJ, et al. Developing consistently reproducible intervertebral disc degeneration at rat caudal spine by using needle puncture. J Neurosurg Spine. 2009; 10:522–530. [PubMed: 19558284]
26. Zhang H, Yang S, Wang L, et al. Time course investigation of intervertebral disc degeneration produced by needle-stab injury of the rat caudal spine: laboratory investigation. J Neurosurg Spine. 2011; 15:404–413. [PubMed: 21721872]
27. Grunert P, Hudson KD, Macielak MR, et al. Assessment of intervertebral disc degeneration based on quantitative magnetic resonance imaging analysis: an in vivo study. Spine (Phila Pa 1976). 2014; 39:E369–378. [PubMed: 24384655]

28. Hsieh AH, Hwang D, Ryan DA, et al. Degenerative anular changes induced by puncture are associated with insufficiency of disc biomechanical function. Spine (Phila Pa 1976). 2009; 34:998–1005. [PubMed: 19404174]
29. Yuan W, Che W, Jiang YQ, et al. Establishment of intervertebral disc degeneration model induced by ischemic sub-endplate in rat tail. Spine Journal: Official Journal of the North American Spine Society. 2015; 15:1050–1059.
30. Martin JT, Gorth DJ, Beattie EE, et al. Needle puncture injury causes acute and long-term mechanical deficiency in a mouse model of intervertebral disc degeneration. J Orthop Res. 2013; 31:1276–1282. [PubMed: 23553925]
31. Ohnishi T, Sudo H, Iwasaki K, et al. In Vivo Mouse Intervertebral Disc Degeneration Model Based on a New Histological Classification. PLoS ONE. 2016; 11:e0160486. [PubMed: 27482708]
32. Yang F, Leung VY, Luk KD, et al. Injury-induced sequential transformation of notochordal nucleus pulposus to chondrogenic and fibrocartilaginous phenotype in the mouse. J Pathol. 2009; 218:113–121. [PubMed: 19288580]
33. Tian Z, Ma X, Yasen M, et al. Intervertebral Disc Degeneration in a Percutaneous Mouse Tail Injury Model. Am J Phys Med Rehabil. 2018; 97:170–177. [PubMed: 28863006]
34. Liang H, Ma SY, Feng G, et al. Therapeutic effects of adenovirus-mediated growth and differentiation factor-5 in a mice disc degeneration model induced by annulus needle puncture. Spine Journal: Official Journal of the North American Spine Society. 2010; 10:32–41.
35. Gullbrand SE, Ashinsky BG, Martin JT, et al. Correlations between quantitative T2 and T1rho MRI, mechanical properties and biochemical composition in a rabbit lumbar intervertebral disc degeneration model. J Orthop Res. 2016; 34:1382–1388. [PubMed: 27105019]
36. Martin JT, Collins CM, Ikuta K, et al. Population average T2 MRI maps reveal quantitative regional transformations in the degenerating rabbit intervertebral disc that vary by lumbar level. J Orthop Res. 2015; 33:140–148. [PubMed: 25273831]
37. Lin KH, Tang SY. The Quantitative Structural and Compositional Analyses of Degenerating Intervertebral Discs Using Magnetic Resonance Imaging and Contrast-Enhanced Micro-Computed Tomography. Ann Biomed Eng. 2017; 45:2626–2634. [PubMed: 28744842]
38. Marinelli NL, Haughton VM, Munoz A, et al. T2 relaxation times of intervertebral disc tissue correlated with water content and proteoglycan content. Spine (Phila Pa 1976). 2009; 34:520–524. [PubMed: 19247172]
39. Perry J, Haughton V, Anderson PA, et al. The value of T2 relaxation times to characterize lumbar intervertebral disks: preliminary results. AJNR Am J Neuroradiol. 2006; 27:337–342. [PubMed: 16484406]
40. Wang YX, Zhao F, Griffith JF, et al. T1rho and T2 relaxation times for lumbar disc degeneration: an in vivo comparative study at 3.0-Tesla MRI. Eur Radiol. 2013; 23:228–234. [PubMed: 22865227]
41. Gullbrand SE, Malhotra NR, Schaer TP, et al. A large animal model that recapitulates the spectrum of human intervertebral disc degeneration. Osteoarthritis Cartilage. 2017; 25:146–156. [PubMed: 27568573]

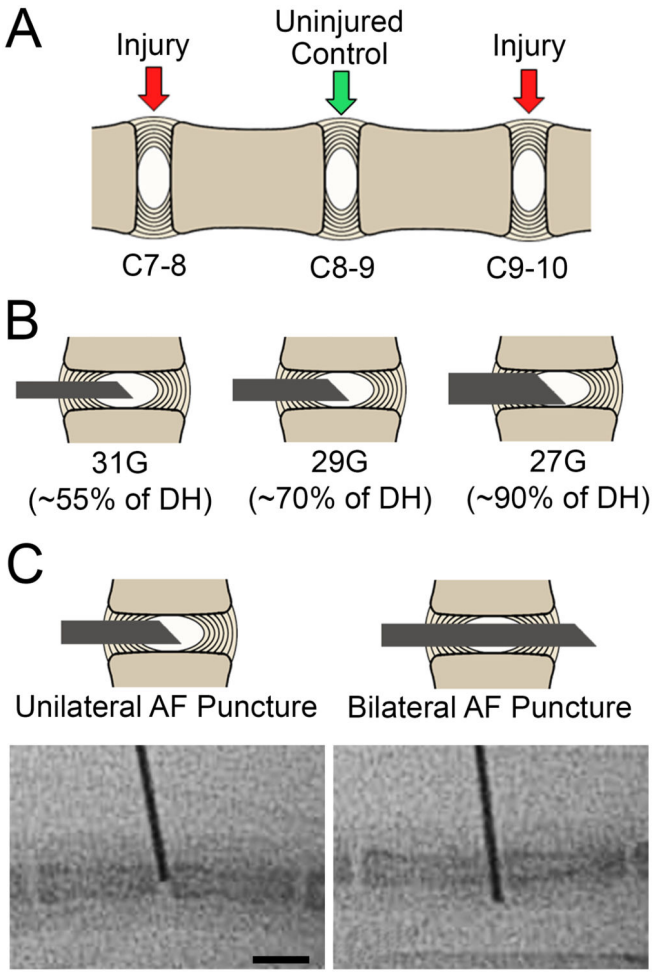

Figure 1.

A. Schematic representation of the mouse caudal spine showing the three experimental disc levels. **B.** Schematic representations of the three needle sizes used for disc injury. **C.** Schematic representations and corresponding intraoperative fluoroscopy images (below), showing the two injury types investigated for each needle size (unilateral or bilateral AF puncture). Scale = 5 mm.

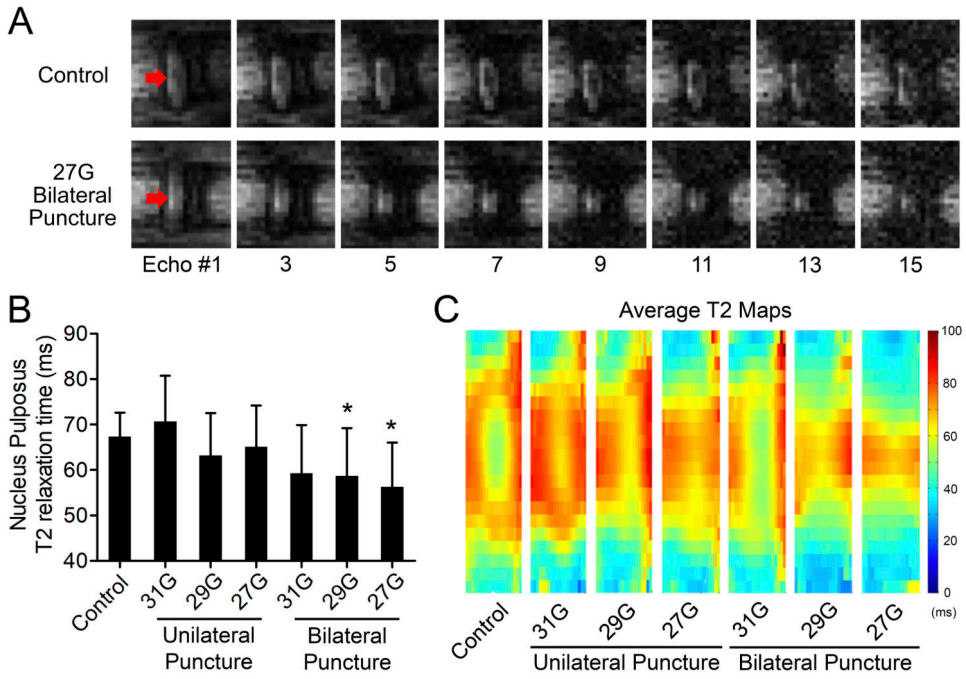

Figure 2.

Magnetic resonance imaging. **A.** Representative echoes illustrating T2 relaxation times for a control disc and a disc that received a bilateral injury with a 27G needle. Arrows indicate the location of the NP. **B.** Effects of injury type on NP T2 relaxation time. 29G and 27G bilateral AF puncture injury resulted in significantly lower T2 values compared to control (*$p < 0.05$, mean ± SD). **C.** Population average T2 maps for each experimental group. Note the relatively hypointense region within the central NP of the intervening control that likely reflects the cell dense notochordal remnant.

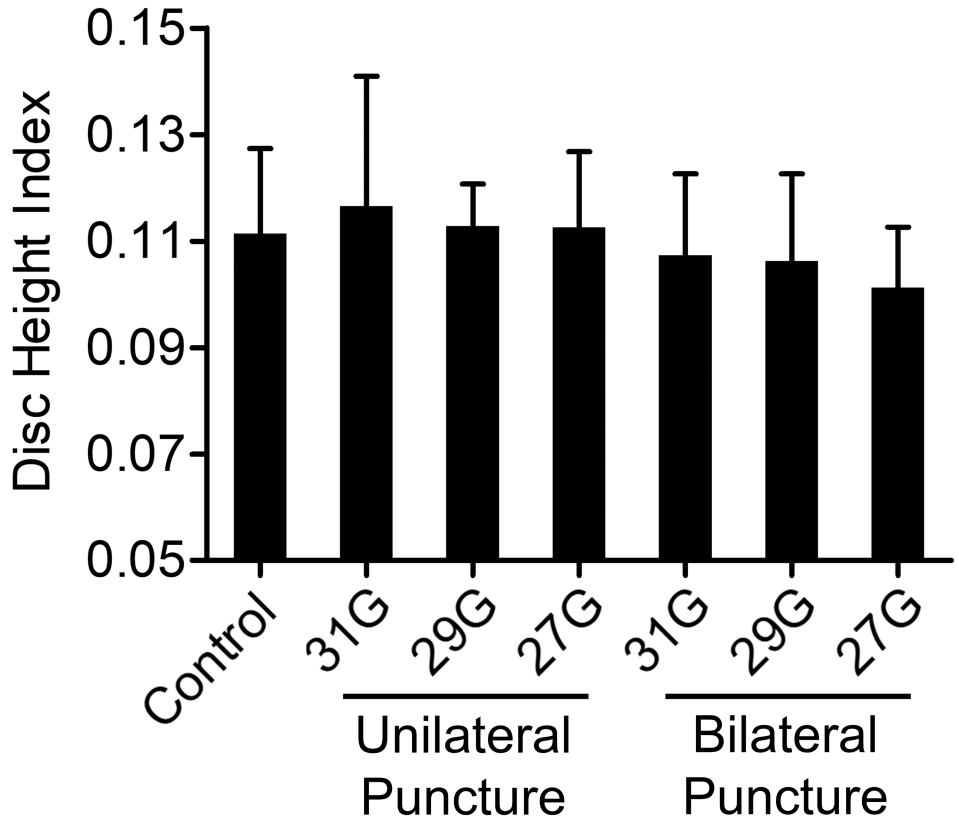

Figure 3.
Disc height index calculated from microcomputed tomography (mean ± SD). There were no differences in disc height index between experimental groups.

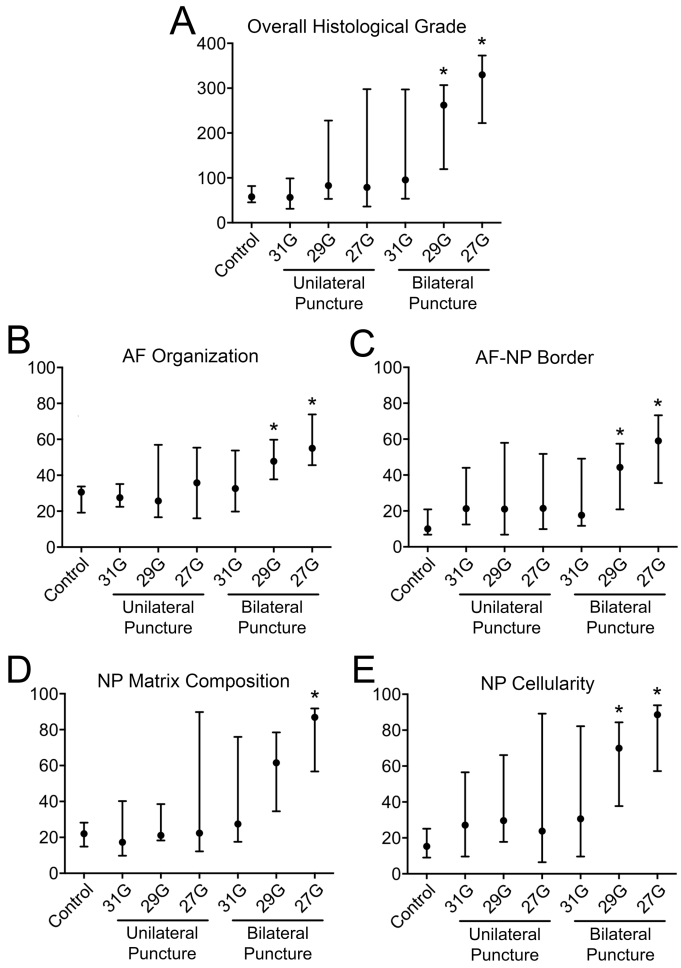

Figure 4.

Semi-quantitative histological assessment of injured disc levels compared with control. **A.** Overall histological grade. **B-E.** Histological subcategory grades. 29G and 27G bilateral puncture groups demonstrated significantly worse histological scores compared with control (overall and all subcategories; median and IQR; *$p < 0.05$ vs control).

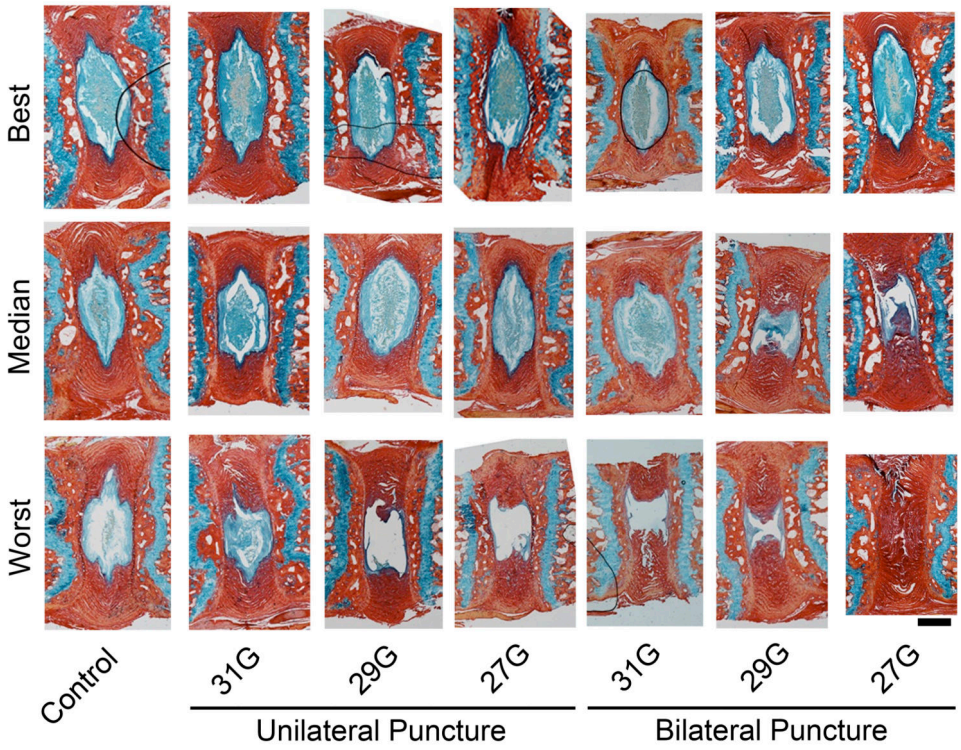

Figure 5.

Representative histology (Alcian blue and picrosirius red staining for glycosaminoglycans and collagen, respectively). Samples with best, median, and worst histological scores for each experimental group are presented. Scale = 300 μm.

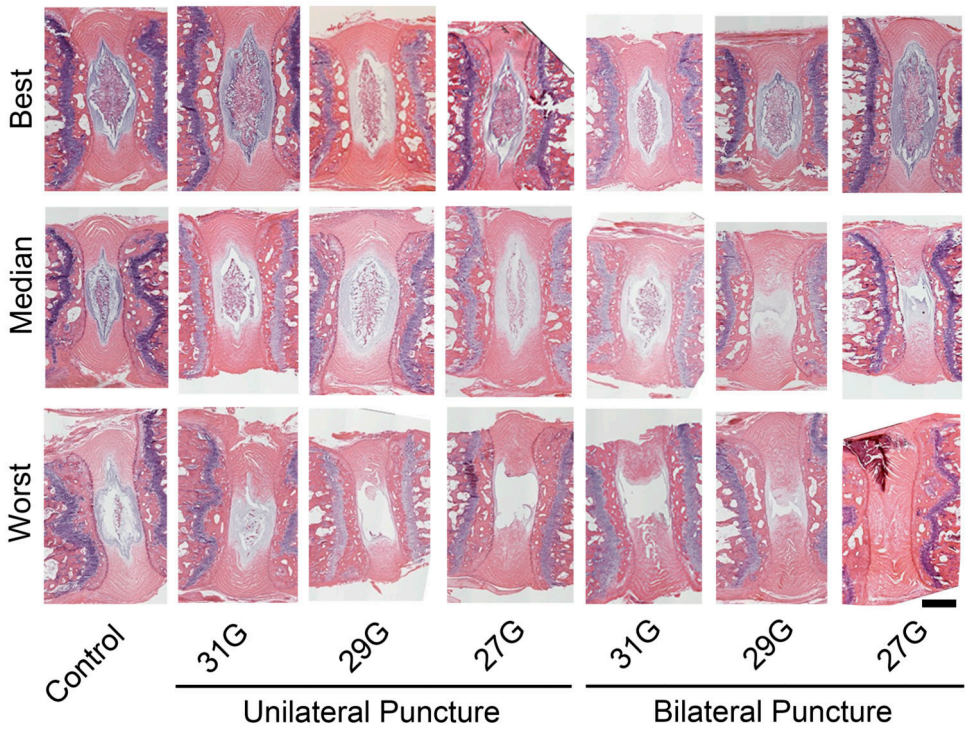

Figure 6.

Representative histology (hematoxylin and eosin staining). Samples with best, median and worst histological scores for each experimental group are presented. Scale = 300 μm.

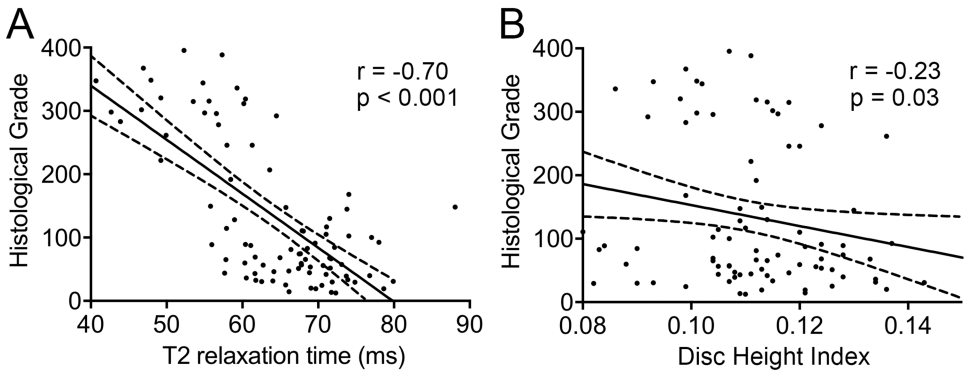

Figure 7.

Correlations between imaging outcomes and histological grade. **A.** Strong, significant, inverse linear correlation between overall histological grade and NP T2 relaxation time. **B.** Weak, significant, inverse linear correlation between overall histological grade and disc height index. Solid and dotted lines represent regression plot and associated 95% confidence intervals respectively.

Table 1

Histological grading criteria

Category	Description
Organization of the Annulus Fibrosus	0 = normal; organized lamellar structure 25 = mild serpentine patterning 50 = mild in-folding and disorganization of lamellae 75 = moderate disorganization of lamellae 100 = severe disorganization and in-folding of lamellae
Annulus Fibrosus/Nucleus Pulposus Border	0 = clear border between the AF and NP 50 = loss of distinction between the AF and NP 100 = border between the AF and NP not discernable
Nucleus Pulposus Extracellular Matrix	0 = gelatinous, proteoglycan rich NP ECM 25 = mild condensation or fragmentation of NP ECM or mild reduction in glycosaminoglycan staining 50 = moderate condensation of NP ECM or moderate reduction in glycosaminoglycan staining 75 = severe NP ECM condensation or fragmentation or severe reduction in glycosaminoglycan staining 100 = Complete absence of glycosaminoglycan staining, marked fibrosis of NP
Nucleus Pulposus Cellularity	0 = many notochordal/chondrocyte-like cells 25 = mild reduction in notochordal/chondrocyte-like cell populations 50 = significant reduction in chondrocyte-like cells 75= rare chondrocyte-like cells, evidence of early fibrosis 100 = fibroblast-like cells with surrounding fibrosis, absence of any chondrocyte-like cells